J. Phase Equilib. Diffus. (2020) 41:870–882
https://doi.org/10.1007/s11669-020-00850-0

Thermodynamic Description of the C-Cr-Zr System Over the Whole Composition and Temperature Ranges

Yafei Pan[1,2] · Lei Huang[1,2] · Jiuxing Zhang[1,2] · Yong Du[3] · Fenghua Luo[3] · Shuyan Zhang[4]

Submitted: 29 July 2020 / in revised form: 23 October 2020 / Accepted: 27 October 2020 / Published online: 9 November 2020

Abstract The thermodynamic modeling of the ternary system C-Cr-Zr has been obtained by modeling the Gibbs energy of all individual phases using the CALPHAD (CALculation of PHAse Diagrams) approach. There is no ternary compound in this system. The liquid is modeled as a substitutional solution phase, while the solid solution phases including ZrC, (αZr), (βCr), (βZr), Cr_3C_2, Cr_7C_3, $Cr_{23}C_6$, C14, C15 and C36 are described by sublattice models. The modeling covers the whole composition and temperature ranges. A set of self-consistent thermodynamic parameters for the C-Cr-Zr system is obtained by considering the phase diagram data in the ternary system. Comprehensive comparisons between the calculated and measured phase diagram and thermodynamic data show that the experimental information is satisfactorily accounted for by the present thermodynamic description. The liquidus projection and reaction scheme of the C-Cr-Zr system are also presented.

Keywords C-Cr-Zr · CALPHAD · phase equilibria · thermodynamic modeling

1 Introduction

By introducing refractory metal elements such as Cr and Zr into carbon steel, dispersed carbides can be formed during the aging process, so as to obtain excellent mechanical properties and heat-resistance.[1,2] In addition, Cr- and Zr-based carbides are also identified as the effective reinforcing particles to fabricate the outstanding cutting tools. It has been proven that ZrC can significantly improve the hardness and high-temperature properties of WC-based cemented carbides.[3] The introduce of Cr_3C_2 to the TiC-based cermets can not only facilitate the formation of finer microstructure and better mechanical performance, but also improve their ability of oxidation resistance, rust resistance and corrosion resistance.[4] Thus, it is of technological interest to study the formation of the carbides in the C-Cr-Zr system.

The CALPHAD (CALculation of PHAse Diagrams) approach is a useful tool to establish thermodynamic databases, which are the bases for the prediction of thermodynamic properties, phase diagrams, diffusion[5] and phase-field simulations.[6] In order to develop the thermodynamic databases of multicomponent cemented carbides,[7] knowledge concerning phase equilibria and thermodynamic properties of the C-Cr-Zr ternary system is of fundamental importance. The present work is thus intended to (I) critically evaluate the experimental phase

✉ Yafei Pan
pan2018@hfut.edu.cn

✉ Shuyan Zhang
Shuyan.zhang@ceamat.com

1 School of Materials Science and Engineering, Hefei University of Technology, Hefei, Anhui 230009, People's Republic of China

2 Engineering Research Center of High Performance Copper Alloy Materials and Processing, Ministry of Education, Hefei University of Technology, Hefei 230009, Anhui, People's Republic of China

3 State Key Laboratory of Powder Metallurgy, Central South University, Changsha 410083, Hunan, People's Republic of China

4 Centre of Excellence for Advanced Materials, Songshan Lake, Dongguan 523808, Guangdong, People's Republic of China

diagram information and thermodynamic data in the C-Cr-Zr ternary system and its constituent binary systems from the literature, and (II) develop self-consistent thermodynamic description for the C-Cr-Zr system by means of the CALPHAD approach.

2 Evaluation of Phase Diagram Data in the Literature

In the present assessment, the published phase diagram, and thermodynamic data of C-Cr-Zr system are critically reviewed. To facilitate reading, the symbols to denote the stable phases in the C-Cr-Zr system are summarized in Table 1.

2.1 Binary Systems

The thermodynamic descriptions of the C-Cr binary system were firstly performed by Andersson[8] and Kajihara and Hillert.[9] However, the thermodynamic parameters obtained by these two groups of authors, could not meet the demand for a reasonable extrapolation to the Fe-Cr-V-C system. Consequently, Lee[10] reassessed the C-Cr system by considering both the C-Cr-Ni and Fe-Cr-V-C systems. Most recently, Khvan et al.[11] found that the calculated temperature of the eutectic reactions in the C-Cr system by using the parameters from Lee's work[10] is even lower than the reported temperature of the corresponding ternary eutectic reaction.[12] For this reason, they reassessed the parameters of the liquid phase in C-Cr system on the basis of absorbing other solid phase parameters from Lee.[10] As discussed above, the modeling reported by Khvan et al.[11] is adopted in the present work.

The thermodynamic description from Guillermet[13] is generally admitted as the major contribution on the C-Zr binary system, which proposed a reliable assessment of the system based on a wide compilation of experimental data from previous works.[14–17] In the present optimization, the description of the C-Zr system derives from Guillermet's work,[13] which has been widely used in the thermodynamic database of cemented carbides.

Many researchers have performed thermodynamic modeling of the Cr-Zr system.[18–20] Recently, Pavlů et al.[21] carried out the first-principles calculations on the total energies of Laves phases in all three structures, i.e. C14, C15 and C36. Then they derived a thermodynamic description of the Cr-Zr system based on the calculation results. In addition, Lu et al.[22] performed the experimental study at different temperatures to determine the phase boundaries and supplemented the literature with new experimental and calculated data to re-evaluate the Cr-Zr system. On the basis of the work form Lu et al.[22] Liu et al.[23] conducted a modified description of the C15 phase and adjusted the invariant reaction from C36 = C15 + L (1547 °C) to L + C36 = C15 (1562 °C), in order to better fit the phase relationships in the Cu-Cr-Zr ternary system. The parameters of Cr-Zr system are adopted from the works of Lu et al.,[22] and Liu et al.[23]

2.2 Ternary Systems

The first investigation on the phase equilibria of the C-Cr-Zr system was reported by Fedorov and Kuz'ma[24] at 1300 °C. The isothermal section is characterized by the ZrC phase with a NaCl-type crystalline structure, which forms six three-phase regions: ZrC + (C) + Cr_3C_2, ZrC + Cr_3C_2 + Cr_7C_3, ZrC + Cr_7C_3 + $Cr_{23}C_6$,

Table 1 Crystallographic information and thermodynamic models to describe the phases in the C-Cr-Zr system

Phase	Prototype	Pearson symbol	Space group	Designation	Phase description
Liquid	–	–	–	Liquid,L	Liquid solution
ZrC	NaCl	cF8	*Fm*-3 *m*	ZrC	Solid solution based on fcc ZrC
(βCr) or (βZr)	W	cI2	*Im*-3 *m*	(βCr,βZr)	Solid solution based on bcc (βCr) or (βZr)
(αZr)	Mg	hP2	$P6_3/mmc$	(αZr)	Solid solution based on hcp (αZr)
Cr_3C_2	Cr_3C_2	oP20	*Pnma*	Cr_3C_2	Binary stoichiometric phase of Cr_3C_2
Cr_7C_3	Cr_7C_3	hP80	*P3c1*	Cr_7C_3	Binary stoichiometric phase of Cr_7C_3
$Cr_{23}C_6$	$Cr_{23}C_6$	cF116	*Fm*-3 *m*	$Cr_{23}C_6$	Binary stoichiometric phase of $Cr_{23}C_6$
Cr_2Zr_C14	$MgZn_2$	hP12	$P6_3/mmc$	C14	Solid solution based on Laves_C36 Cr_2Zr
Cr_2Zr_C15	$MgCu_2$	cF24	*Fd*-3 *m*	C15	Solid solution based on Laves_C15 Cr_2Zr
Cr_2Zr _C36	$MgNi_2$	hP24	$P6_3/mmc$	C36	Solid solution based on Laves_C36 Cr_2Zr
Graphite	C-a	hP4	$P6_3/mmc$	Graphite,(C)	Graphite carbon

ZrC + $Cr_{23}C_6$ + (βCr), ZrC + (βCr) + C15 and ZrC + C15 + (βZr). The solubility of Cr in the ZrC reaches up to 6 at.%, while Cr-based carbides dissolve negligible amounts of Zr. It should be noted that the phase boundaries of the three-phase regions were determined by the methods of x-ray diffraction and microstructural analyses and the detailed alloy compositions were not reported in their work. Obviously, their work cannot accurately determine the solubility of Cr in the ZrC phase with different carbon contents. Since the relevant data is very limited, these phase equilibria are also given the certain weight in the present modeling.

The invariant equilibria of the C-Cr-Zr system were investigated by Eremenko et al.[25,26] using chemical analysis (CA), x-ray diffraction (XRD), scanning electron microscopy (SEM), differential thermal analysis (DTA) and Pirani-Alterthum method. The investigated specimens were prepared by arc-melting, followed by homogenization treatment. The primary crystallization phases, namely those of ZrC, Cr_3C_2, Cr_7C_3, $Cr_{23}C_6$, (βCr), (βZr), C14 and (C) are detected in the as-cast alloys. Eremenko et al.[26] given the invariant equilibria of L + (C) = ZrC + Cr_3C_2 at 1805 °C, L = ZrC + Cr_3C_2 + Cr_7C_3 at 1730 °C, L + Cr_7C_3 = ZrC + $Cr_{23}C_6$ at 1605 °C, L = ZrC + $Cr_{23}C_6$ + (βCr) at 1575 °C, L = ZrC + (βCr) + C14 at 1595 °C, and L = ZrC + C14 + (βZr) at 1320 °C. They also reported three ternary eutectic maxima reactions, i.e., L = ZrC + Cr_7C_3 at 1750 ± 10 °C, L = ZrC + (βCr) at 1740 ± 10 °C and L = ZrC + C14 at 1630 ± 10 °C.

Based on the obtained thermodynamic data, Eremenko et al.[26] also constructed two vertical sections of $Cr_{75}Zr_{25}$-$Cr_{75}C_{25}$ and Zr-$Cr_{52}C_{48}$. Using DTA method, Shurin and Dmitrieva[27] determined the Cr-ZrC vertical section with a eutectic temperature of 1785 ± 20 °C and composition of 4.2 at.% ZrC, which is consistent with the result from Eremenko et al.[26] According to Shurin and Dmitrieva,[27] the solubility of ZrC in (Cr) at 1785 °C is measured to be 1.3 at.%. The data mentioned above are all considered in the present optimization.

3 Thermodynamic Models

In the present modeling, the Gibbs energy functions for the elements C, Cr and Zr are taken from the SGTE compilation by Dinsdale.[28] The thermodynamic parameters in the C-Cr, C-Zr and Cr-Zr binary sub-systems are taken from Khvan et al.,[11] Guillermet,[13] and Liu et al.[23] Different thermodynamic models are applied depending on the crystal structure and thermodynamic property of each phase.

3.1 Liquid

The liquid phase is described as substitutional solution, and the Gibbs energy is expressed by the Redlich-Kister-Muggianu polynomial[29,30]:

$$\begin{aligned} {}^0G_m^L = {} & x_C \cdot {}^0G_C^L + x_{Cr} \cdot {}^0G_{Cr}^L + x_{Zr} \cdot {}^0G_{Zr}^L \\ & + RT \cdot (x_C \cdot \ln x_C + x_{Cr} \cdot \ln x_{Cr} + x_{Zr} \cdot \ln x_{Zr}) \\ & + x_C \cdot x_{Cr} \cdot L_{C,Cr}^L + x_C \cdot x_{Zr} \cdot L_{C,Zr}^L + x_{Cr} \cdot x_{Zr} \cdot L_{Cr,Zr}^L \\ & + {}^{ex}G_{C,Cr,Zr}^L \end{aligned} \quad \text{(Eq 1)}$$

where R is the gas constant, and x_C, x_{Cr} and x_{Zr} are molar fractions of the elements C, Cr and Zr, respectively. The standard element reference (SER) state,[28] i.e. the stable structure of the element at 25 °C and 1 bar, is used as the reference state of Gibbs energy. The parameters $L_{i,j}^L\,(i,j = C, Cr, Zr)$ are the interaction parameters from the binary constituent systems. The ternary excess Gibbs energy ${}^{ex}G_{C,Cr,Zr}^L$ is expressed as follows:

$${}^{ex}G_{C,Cr,Zr}^L = x_C \cdot x_{Cr} \cdot x_{Zr} \cdot \left(x_C \cdot {}^0L_{C,Cr,Zr}^L + x_{Cr} \cdot {}^1L_{C,Cr,Zr}^L + x_{Zr} \cdot {}^2L_{C,Cr,Zr}^L\right) \quad \text{(Eq 2)}$$

in which the interaction parameters ${}^0L_{C,Cr,Zr}^L$, ${}^1L_{C,Cr,Zr}^L$ and ${}^2L_{C,Cr,Zr}^L$ are linearly temperature-dependent. These parameters will be evaluated in the present work.

3.2 Solid Solution Phases

The Gibbs energies of the ZrC, (βCr), (βZr) and (αZr) phases are described using two-sublattice models developed by Hillert and Staffansson[31] as $(Cr, Zr)_a(C, Va)_c$. In this model, it is assumed that Cr and Zr atoms occupy one sublattice while C atoms and vacancies occupy the other one, since C atoms are generally known to occupy only interstitial sites in these phases. The symbols a and c denote the numbers of sites on each sublattice and have values of a = 1 and c = 1 for the ZrC phase with fcc structure; a = 1 and c = 3 for the (βCr)) and (βZr) phases with bcc structure; a = 1 and c = 0.5 for the (αZr) phase with hcp structure. For one formula unit $(Cr, Zr)_a(C, Va)_c$, the Gibbs energy of a phase is expressed as follows:

$$
\begin{aligned}
G_m^{\varphi} = {} & y'_{Cr} \cdot y''_C \cdot {}^0G^{\varphi}_{Cr:C} + y'_{Zr} \cdot y''_C \cdot {}^0G^{\varphi}_{Zr:C} + y'_{Cr} \cdot y''_{Va} \cdot {}^0G^{\varphi}_{Cr:Va} \\
& + y'_{Zr} \cdot y''_{Va} \cdot {}^0G^{\varphi}_{Zr:Va} + a \cdot RT \cdot (y'_{Cr} \cdot \ln y'_{Cr} + y'_{Zr} \cdot \ln y'_{Zr}) \\
& + c \cdot RT \cdot (y''_C \cdot \ln y''_C + y''_{Va} \cdot \ln y''_{Va}) \\
& + y'_{Cr} \cdot y'_{Zr} \cdot y''_C \cdot L^{\varphi}_{Cr,Zr:C} + y'_{Cr} \cdot y'_{Zr} \cdot y''_{Va} \cdot L^{\varphi}_{Cr,Zr:Va} \\
& + y'_{Cr} \cdot y''_C \cdot y''_{Va} \cdot L^{\varphi}_{Cr:C,Va} \\
& + y'_{Zr} \cdot y''_C \cdot y''_{Va} \cdot L^{\varphi}_{Zr:C,Va} + y'_{Cr} \cdot y'_{Zr} \cdot y''_C \cdot y''_{Va} \cdot L^{\varphi}_{Cr,Zr:C,Va}
\end{aligned}
\quad \text{(Eq 3)}
$$

where y'_C and y'_{Zr} are the site fractions of Cr and Zr in the first sublattice, and y''_C and y''_{Va} are the site fractions of C and Va in the second sublattice. The parameter ${}^0G^{\varphi}_{i:Va}$ ($i = Cr$ or Zr) is the Gibbs energy of pure element i, and the parameter ${}^0G^{\varphi}_{i:C}$ ($i = Cr$ or Zr) is the Gibbs energy of a hypothetical state where all the interstitial sites are completely filled with C. $L^{\varphi}_{Cr,Zr:Va}$, $L^{\varphi}_{Cr:C,Va}$ and $L^{\varphi}_{Zr:C,Va}$ are the binary parameters from the sub-binary systems, while the $L^{\varphi}_{Cr,Zr:C}$ and $L^{\varphi}_{Cr,Zr:C,Va}$ are the ternary parameters that will be optimized in the present assessment.

Considering the limited experimental data on the solubility of the third element, the binary phases Cr_3C_2, Cr_7C_3, $Cr_{23}C_6$, C14, C15 and C36 are considered as pure binary stoichiometric phases. It is presumed that the sublattice of graphite is totally filled by C due to the negligible solubility of Cr and Zr in graphite. The Gibbs energy of graphite is taken from the SGTE database.[28]

4 Results and Discussion

The evaluation of the model parameters was carried out using the optimization program PARROT,[32] which works by minimizing the sum of the square of the differences between measured and calculated values. The step-by-step optimization procedure described by Du et al.[33] was utilized in the present assessment. Each piece of selected information was given a certain weight based on the uncertainties of the experimental data. The weights were changed by trial and error during the assessment until most of the selected experimental information was reproduced within the expected uncertainty limits.

Based on the experimental sections of 1300 °C,[24] the modeling of the C-Cr-Zr system proceeds with the solid phase. Therefore, the thermodynamic parameters of ZrC phase are firstly evaluated. For the fcc-ZrC phase with large homogeneity ranges varying from 37.3 to 50.0 at.% C, two ternary parameters ${}^0L^{Fcc}_{Cr,Zr:C}$ and ${}^2L^{Fcc}_{Cr,Zr:C}$ are introduced to model the ZrC with higher C contents, while one ternary parameters ${}^1L^{Fcc}_{Cr,Zr:C,Va}$ are adopted to model the ZrC with lower C contents. During the optimization, it is found that the parameter ${}^0G^{Fcc}_{Cr,Zr:C}$ is used to limit the solid solubility of Cr in the ZrC phase. When the parameter ${}^0G^{Fcc}_{Cr,Zr:C}$ reaches up to +161,903.988, the solubility solid solubility of Cr in the ZrC phase is reduced to 7.35 at.%. The parameter ${}^2G^{Fcc}_{Cr,Zr:C}$ is used to increase the stability of the ZrC phase. Only by setting the parameter to − 323,421.99 or below, the assessment can fit well with the experimental data and avoid the formation of fcc#1 + fcc#2 for the ZrC phase in the high C region. No ternary parameters of (αZr) with hcp structure and (βCr) and (βZr) with bcc structure are introduced in the present assessment. Subsequently, ${}^0L^{Liquid}_{C,Cr,Zr}$ and ${}^2L^{Liquid}_{C,Cr,Zr}$ for liquid are assessed by using the experimental data including liquidus, primary crystallization fields and invariant equilibria.[25,26] The parameter ${}^0L^{Liquid}_{C,Cr,Zr}$ is mainly to assess the temperatures of the invariant reactions related to the C-Cr binary system and the parameter ${}^2L^{Liquid}_{C,Cr,Zr}$ is mainly to assess the temperatures of the invariant reactions related to the Cr-Zr binary system. Finally, the thermodynamic parameters obtained above are optimized at the same time by considering all selected phase diagram information.

Table 2 presents the thermodynamic parameters of the C-Cr-Zr system obtained from the present modeling. Based on these thermodynamic parameters, all phase equilibrium data are calculated to demonstrate the reasonability of the present assessment including isothermal sections, vertical sections and liquidus projection (Fig. 1).

The calculated sections of the C-Cr-Zr system at 1300 °C in comparison with the experimental results from Fedorov and Kuz'ma[24] are shown in Fig. 2. It can be seen that the calculated phase relationships fit well with the experimental ones. The ZrC phase forms six three-phase regions with the (C), Cr_3C_2, Cr_7C_3, $Cr_{23}C_6$, (βCr), C15 and (βZr) phases. The maximum solid solubility of Cr in ZrC is calculated to be 7.35 at.%, which occurs at 47.2 at.% C. In the present modeling, the solubilities of Zr in the Cr_3C_2, Cr_7C_3 and $Cr_{23}C_6$ phases and C in the C15 phase is set to be zero, which is very close to the experimental results.

To better illuminate the phase relationship of the C-Cr-Zr system, Fig. 3a–f shows the calculated sections at 500, 1500, 1600, 1700, 2000 and 3000 °C. It can be seen that the solubility of Cr in the ZrC phase does not change significantly with the increasing temperature. The liquid phase firstly forms in the Zr-rich corner and gradually extends to the whole Cr-Zr sub-binary side, as the

Table 2 Summary of the optimized thermodynamic parameters in the C-Cr-Zr system[a]

Liquid: Model (C,Cr, Zr)$_1$

$^0L^{Liquid}_{C,Cr} = -69245 - 35T$ | $^0L^{Liquid}_{C,Cr} = +83242$ | $^0L^{Liquid}_{C,Cr} = +88000$

$^0L^{Liquid}_{C,Zr} = -305420.6 - 16.02T$ | $^0L^{Liquid}_{C,Zr} = -39269.66$ | $^2L^{Liquid}_{C,Zr} = +50000$

$^0L^{Liquid}_{Cr,Zr} = -10071.34 - 1.20T$ | $^1L^{Liquid}_{Cr,Zr} = -1425.96 - 0.74T$ | $^0L^{Liquid}_{Cr,Zr} = -8284.87 + 0.92T$

$^0L^{Liquid}_{C,Cr,Zr} = -\underline{731523.70}$ | $^2L^{Liquid}_{C,Cr,Zr} = -\underline{188951.43}$

ZrC: Model (Cr,Zr)$_1$(C,Va)$_1$

$^0G^{Fcc}_{Cr:C} = {}^0G^{Bcc}_{Cr} + {}^0G^{Gra}_{C} + 1200 - 1.94T$

$^0G^{Fcc}_{Zr,C} = -224784.9 + 297.0288T - 48.14055T\ln(T) - 0.001372273T^2 - 1.015994 \times 10^{-7}T^3 + 517213T^{-1} - 8.30054316 \times 10^8T^{-3}$

$^0G^{Fcc}_{Cr:C,Va} = -11977 + 6.8194T$

$^0G^{Fcc}_{Zr:C,Va} = -41870.2 - 35.70271T + 6.042424T\ln(T) - 0.001326472T^2$

$^0G^{Fcc}_{Zr:C,Va} = -81870.2 - 35.70271T + 6.042424T\ln(T) - 0.001326472T^2$

$^0G^{Fcc}_{Cr,Zr:C} = +\underline{161903.988}$ | $^2G^{Fcc}_{Cr,Zr:C} = -\underline{323421.995}$

$^1G^{Fcc}_{Cr,Zr:C,Va} = -\underline{1541197.15}$

(βCr,βZr)-Bcc: Model (Cr,Zr)$_1$(C,Va)$_3$

$^0G^{Bcc}_{Cr:C} = {}^0G^{Bcc}_{Cr} + 3\ {}^0G^{Gra}_{C} + 416000 {}^0G^{Bcc}_{Cr:C} = {}^0G^{Bcc}_{Cr} + 3\ {}^0G^{Gra}_{C} + 416000$

$G^{Bcc}_{Zr,C} = -142838.2 + 631.7121T - 96.28173T\ln(T) - 0.001856037T^2 - 9.2968513 \times 10^{-8}T^3 + 2261356T^{-1} - 7.933899 \times 10^9T^{-3}$

$^0G^{Bcc}_{Cr:C,Va} = -190T$ | $^0G^{Bcc}_{Zr:C,Va} = -223221.3$

$^0G^{Bcc}_{Cr,Zr:Va} = +48365.47–13.9T$ | $^1G^{Bcc}_{Cr,Zr:Va} = +10065.57 - 6.1T$

(αZr)-Hcp: Model (Cr,Zr)$_1$(C,Va)$_{0.5}$

$^0G^{Hcp}_{Cr:C} = {}^0G^{Hcp}_{Cr} + 0.5\ {}^0G^{Hcp}_{C} - 18504 + 9.4173T - 2.4997T\ln(T) + 0.001386T^2$

$^0G^{Hcp}_{Zr:C} = -115822.7 + 212.2971T - 36.10565T\ln(T) - 0.001375489T^2 - 1.361587 \times 10^{-7}T^3 + 217131T^{-1} - 1.9505689 \times 10^8T^{-3}$

$^0G^{Hcp}_{Cr:C,Va} = +4165$ | $^0G^{Hcp}_{Zr:C,Va} = +3206.881$

$^0G^{Hcp}_{Cr,Zr:Va} = +89700 - 11T$ | $^1G^{Hcp}_{Cr,Zr:Va} = +38800 + 6T$

Cr_3C_2: Model (Cr)$_3$(C)$_2$

$^0G^{Cr3C2}_{Cr:C} = -100823.8 + 530.66989T - 89.6694T\ln(T) - 0.03011188T^2$

Cr_7C_3: Model (Cr)$_7$(C)$_3$

$^0G^{Cr7C3}_{Cr:C} = -201690 + 1103.128T - 190.177T\ln(T) - 0.0578207T^2$

$Cr_{23}C_6$: Model (Cr)$_7$(C)$_3$

$^0G^{Cr23C6}_{Cr:C} = -521983 + 3622.24T - 620.965T\ln(T) - 0.126431T^2$

Cr_2Zr-C14: Model (Cr,Zr)$_2$(Cr,Zr)$_1$

$^0G^{C14}_{Cr:Cr} = 3\ {}^0G^{Bcc}_{Cr} + 83339.0 - 2.3T$ | $^0G^{C14}_{Zr:Zr} = 3\ {}^0G^{Hcp}_{Zr} + 62388.0 - 4.3T$

$^0G^{C14}_{Cr:Zr} = 2\ {}^0G^{Bcc}_{Cr} + {}^0G^{Hcp}_{Zr} - 9050.3 - 11.85T$ | $^0G^{C14}_{Zr:Cr} = {}^0G^{Bcc}_{Cr} + 2\ {}^0G^{Hcp}_{Zr} + 279176.1 - 8.2T$

$^0G^{C14}_{Cr:Cr,Zr} = -22800$ | $^0G^{C14}_{Cr,Zr:Zr} = +27800$

Cr_2Zr-C15: Model (Cr,Zr)$_2$(Cr,Zr)$_1$

$^0G^{C15}_{Cr:Cr} = 3\ {}^0G^{Bcc}_{Cr} + 79374.0 - 2.59T$ | $^0G^{C15}_{Zr:Zr} = 3\ {}^0G^{Hcp}_{Zr} + 81154.0 - 8.33T$

$^0G^{C15}_{Cr:Zr} = 3\ {}^0G^{Bcc}_{Cr} + {}^0G^{Hcp}_{Zr} - 23004.1 - 4.26T$ | $^0G^{C15}_{Zr:Cr} = {}^0G^{Bcc}_{Cr} + 2\ {}^0G^{Hcp}_{Zr} + 303085.2 - 8.46T$

$^0G^{C15}_{Cr:Cr,Zr} = -13641.9$ | $^0G^{C15}_{Cr,Zr:Zr} = +13864.39$

Cr_2Zr-C36: Model (Cr,Zr)$_2$(Cr,Zr)$_1$

$^0G^{C36}_{Cr:Cr} = 3\ {}^0G^{Bcc}_{Cr} + 77859.0 - 6.33T$ | $^0G^{C36}_{Zr:Zr} = 3\ {}^0G^{Hcp}_{Zr} + 69218.7 - 3.44T$

$^0G^{C36}_{Cr:Zr} = 2\ {}^0G^{Bcc}_{Cr} + {}^0G^{Hcp}_{Zr} - 11809.8 - 10.4T$ | $^0G^{C36}_{Zr:Cr} = {}^0G^{Bcc}_{Cr} + 2\ {}^0G^{Hcp}_{Zr} + 228202.8 - 8.51T$

$^0G^{C36}_{Cr:Cr,Zr} = -9540$ | $^0G^{C36}_{Cr,Zr:Zr} = +19750$

C: Model (C)$_1$

[a]All parameters are given in J/mole and temperature (T) in K. The Gibbs energies for the pure elements are taken from the compilation of Dinsdale.[28] The thermodynamic parameters in the C-Cr, C-Zr and Cr-Zr binary sub-systems are taken from Khvan et al.,[11] Guillermet[13] and Liu et al.,[23] respectively. The underlined parameters are assessed in the present work

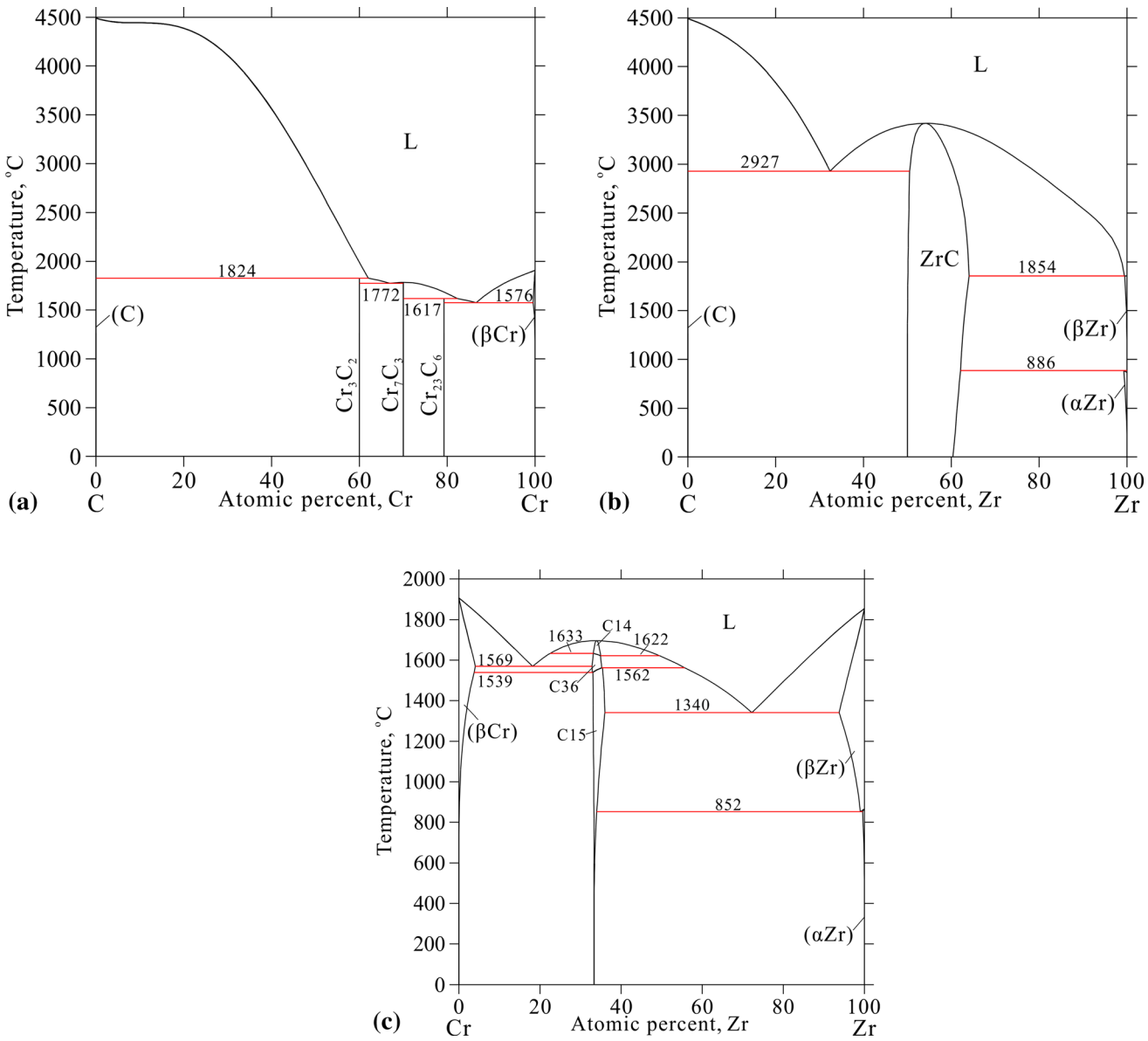

Fig. 1 Calculated binary phase diagrams: (a) C-Cr system, [11] (b) C-Zr system[13] and (c) Cr-Zr system[23]

temperature increases to 2000 °C. In this temperature ranges, the Laves phase undergoes the following transformations: C15 → C36 → C14. When the temperature reaches up to 3000 °C, liquid has dominated the ternary system and the ZrC phase shrinks adjacent to the C-Zr side.

The calculated vertical sections $Cr_{75}Zr_{25}$-$Cr_{75}C_{25}$, Zr-$Cr_{52}C_{48}$ and Cr-$Cr_{60}Zr_{20}C_{20}$ of the C-Cr-Zr system together with the experimental data from Eremenko et al.[26] and Shurin and Dmitrieva[27] are shown in Fig. 4a–c. Most experimental data are in good agreement with the present calculation results. The calculated liquidus projection of the C-Cr-Zr ternary system is given in Fig. 5, while Fig. 6 presents the reaction scheme in the range of melting/solidification for this system. Table 3 presents the

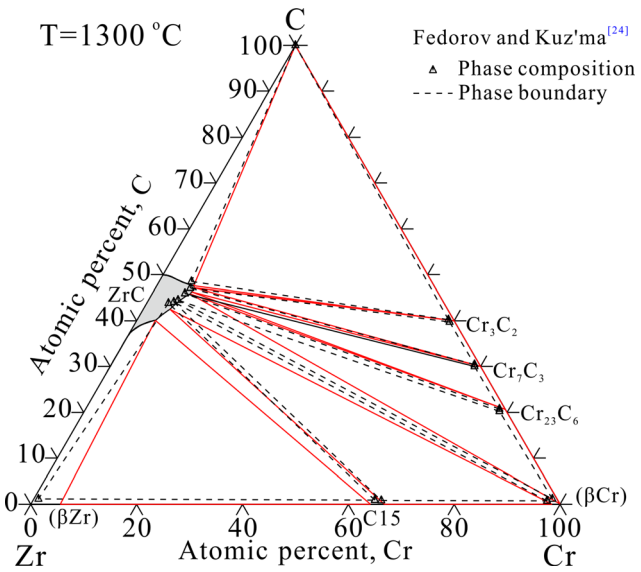

Fig. 2 Calculated isothermal section of the C-Cr-Zr system at 1300 °C compared with the experimental data reported by Fedorov and Kuz'ma[24]

comparison between the calculated and experimental invariant equilibria.[26] The invariant reaction types, temperatures and compositions reported in the literature are well reproduced by the present calculations. Compared with the experimental results reported by Eremenko et al.,[26] the present modeling predicts three primary crystallization regions including one C15 and two C36, and three invariant reactions of U2: L + C14 = ZrC + C36, P1: L + ZrC + C14 = C36 and U4: L + C36 = ZrC + C15.

For the other C-Cr-X (X = Refractory metal elements) systems, the reciprocal parameter of $G^{Fcc}_{Cr,X:C,Va}$ is not adopted to describe the fcc phase in the C-Cr-Ti[34] system, and the reciprocal parameters of $G^{Fcc}_{Cr,X:C,Va}$ are introduced to model the fcc phase in the C-Cr-Ta[35] and C-Cr-Nb[36] systems. Therefore, it is meaningful to discuss the role of the reciprocal parameter $G^{Fcc}_{Cr,X:C,Va}$ in the C-Cr-Zr system. Based on the obtained parameters in the present work, the reciprocal parameter ${}^{1}G^{Fcc}_{Cr,Zr:C,Va}$ for fcc is set to be 0, and the other parameters ${}^{0}G^{Fcc}_{Cr,Zr:C}$ and ${}^{2}G^{Fcc}_{Cr,Zr:C}$ are remodeled and changed from + 161,903.988 and − 323,421.995 to + 50,558.5 and − 429,563.4, respectively. Using the remodeled parameters, the isothermal section of 1300 °C and the Cr-ZrC vertical section are represented in Fig. 7a and b. It can be found the phase relationship is consistent with the previous results, however the phase equilibria information related to ZrC phase cannot be described very well. So it is meaningful to introduce the reciprocal parameter of $G^{Fcc}_{Cr,X:C,Va}$ to model the fcc phase in the C-Cr-Zr system.

5 Conclusions

On the basis of sufficient experimental information, the C-Cr-Zr ternary system is modeled using the CALPHAD method, and a set of reasonable parameters for each phase

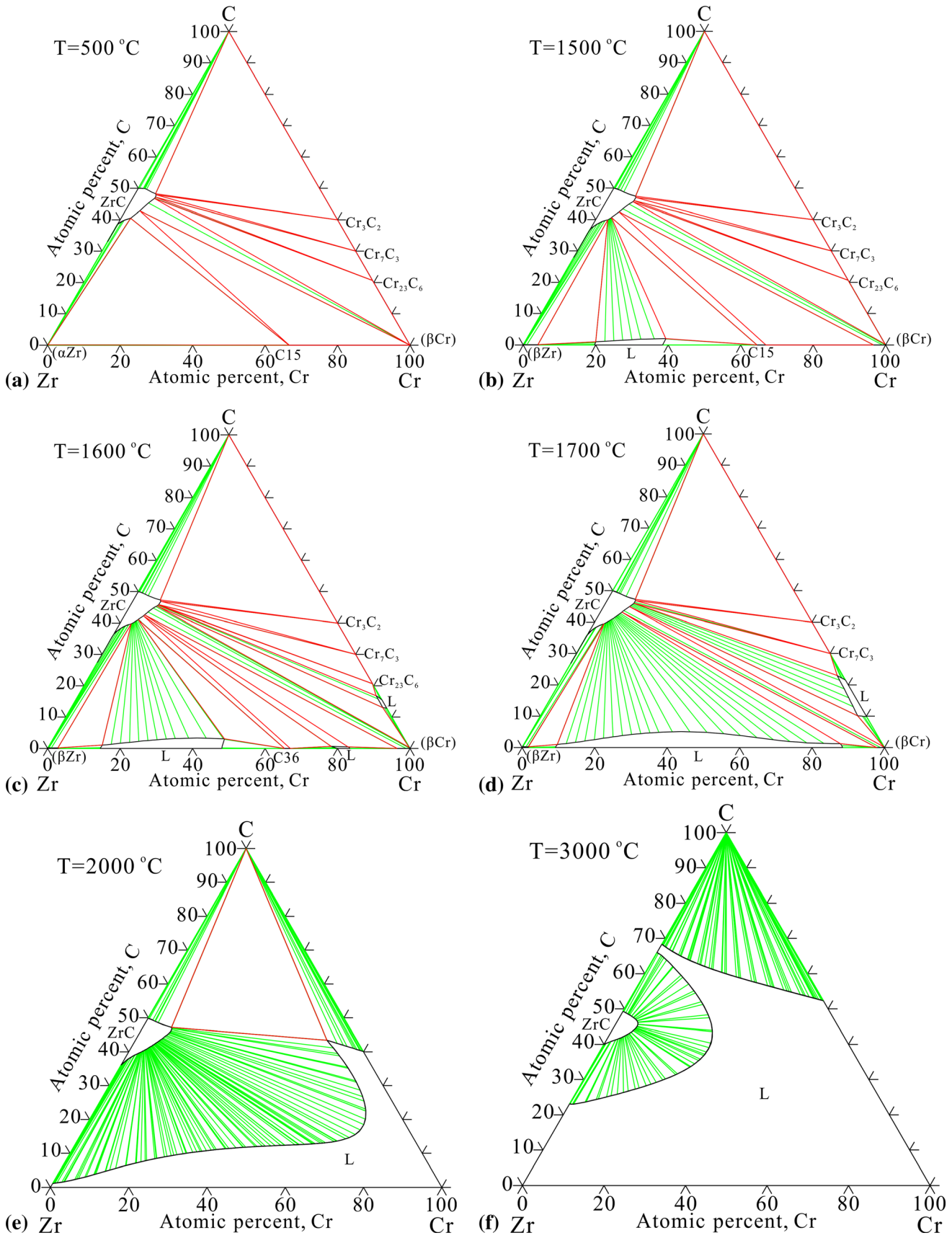
T=500 °C
T=1500 °C
T=1600 °C
T=1700 °C
T=2000 °C
T=3000 °C
C
Zr
Cr
Atomic percent, C
Atomic percent, Cr
ZrC
Cr_3C_2
Cr_7C_3
$Cr_{23}C_6$
(αZr)
(βZr)
(βCr)
C15
C36
L
(a) Zr
(b) Zr
(c) Zr
(d) Zr
(e) Zr
(f) Zr

◀**Fig. 3** Calculated isothermal section of the C-Cr-Zr system at 500 °C (a), 1500 °C (b), 1600 °C (c), 1700 °C (d), 2000 °C (e) and 3000 °C (f)

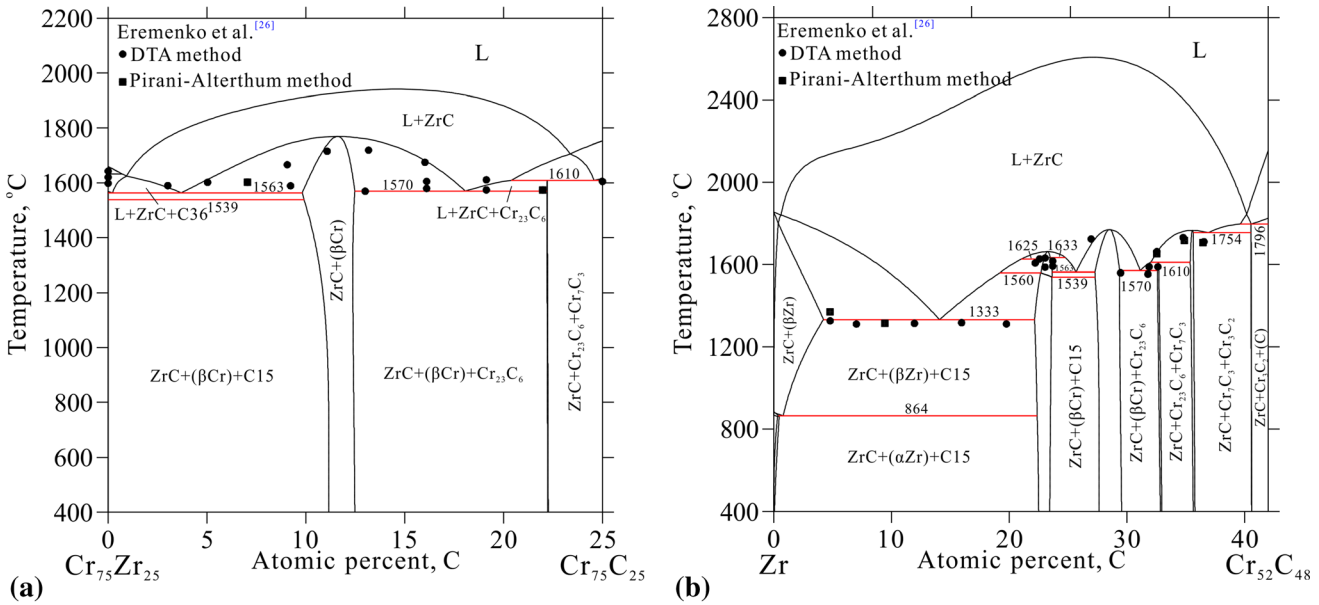

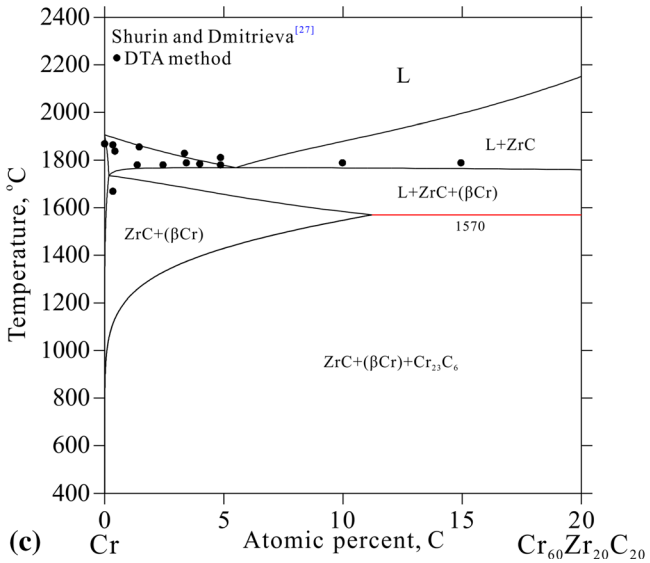

Fig. 4 Calculated vertical sections $Cr_{75}Zr_{25}$-$Cr_{75}C_{25}$, Zr-$Cr_{52}C_{48}$ and Cr-$Cr_{60}Zr_{20}C_{20}$ of the C-Cr-Zr system together with the experimental data from Eremenko et al.[26] and Shurin and Dmitrieva[27]

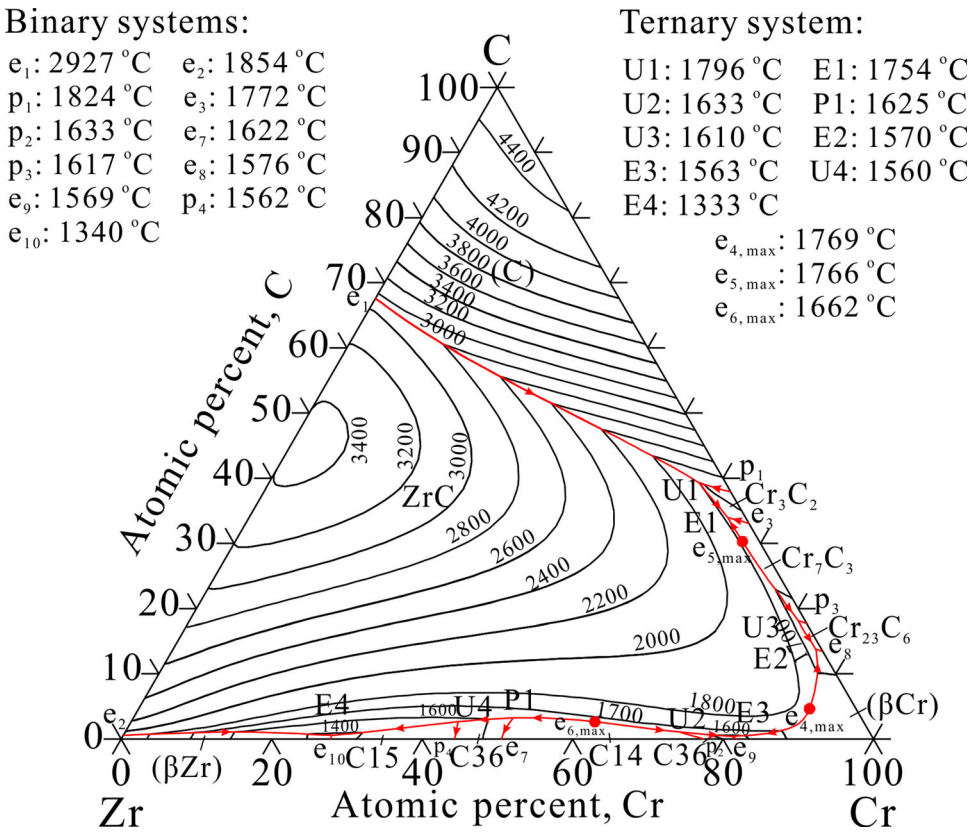

Fig. 5 Calculated liquidus projection of the C-Cr-Zr system according to the present thermodynamic modeling

in this system are obtained, which can well reproduce the phase equilibrium relationships of the ternary system over the whole composition and temperature ranges including vertical sections, isothermal sections and invariant reactions. The liquidus projection and reaction scheme of C-Cr-Zr system are also calculated according to the present optimization, which is very important for practical applications and basic material research.

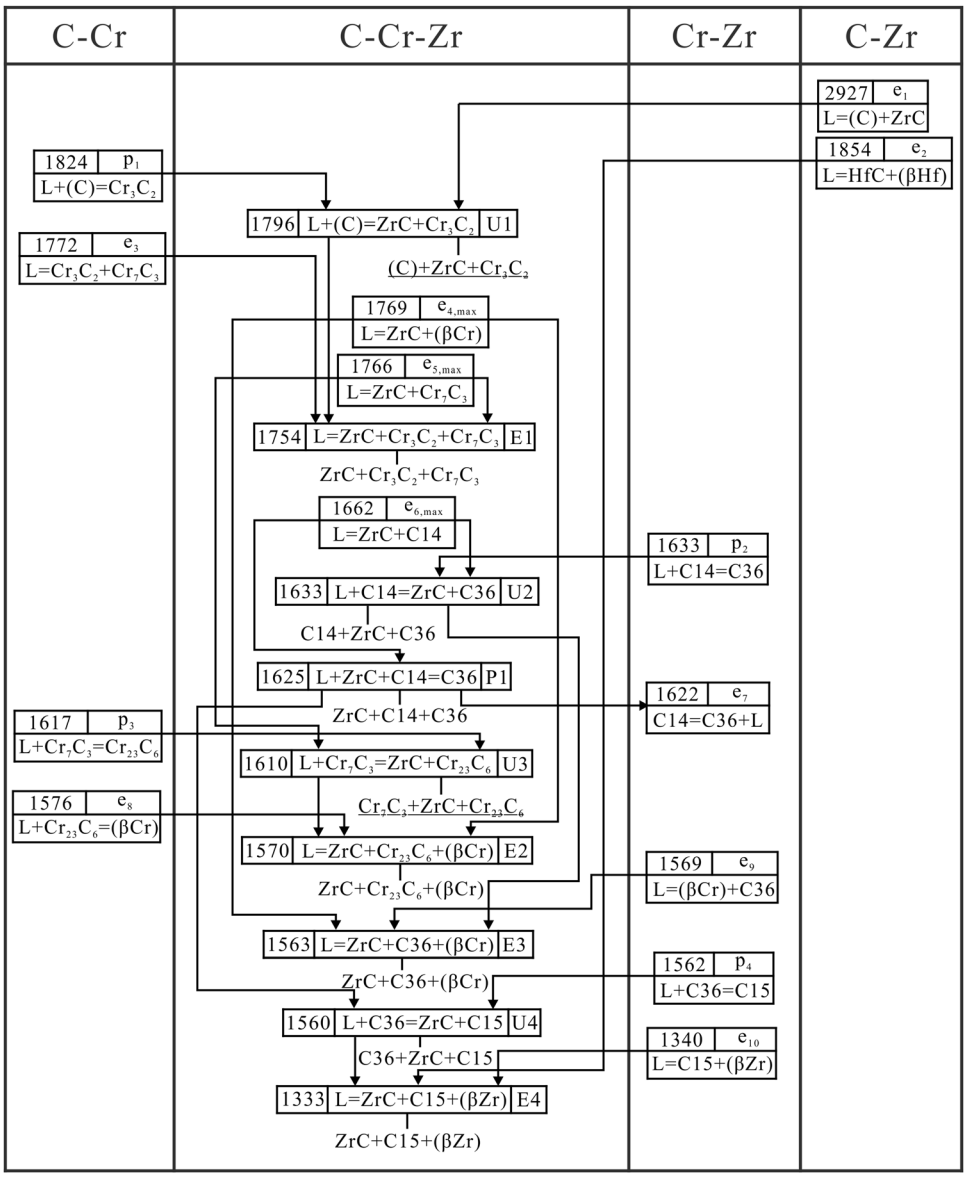

Fig. 6 The reaction scheme for the C-Cr-Zr system including liquid phase according to the present calculations with temperature in °C. The invariant reactions among solid phases are not included in this figure

Table 3 Comparison between the calculated and measured[26] invariant reactions with participation of liquid phase in the C-Cr-Zr system

Invariant reaction	Composition of liquid phase, at.%			T, °C	
	C	Cr	Zr	Cal.	Exp.
$e_{4,max}$: L = ZrC + (βCr)	4.7	89.2	6.1	1769	1740 ± 10
$e_{5,max}$: L = ZrC + Cr_7C_3	30.3	67.4	2.3	1766	1750 ± 10
$e_{6,max}$: L = ZrC + C14	2.6	61.7	35.7	1662	1630 ± 10
U1: L + (C) = ZrC + Cr_3C_2	39.2	57.3	3.5	1796	1805
E1: L = ZrC + Cr_3C_2 + Cr_7C_3	34.0	63.7	2.3	1754	1730
U2: L + C14 = ZrC + C36	1.1	73.7	25.2	1633	–
P1: L + ZrC + C14 = C36	3.2	50.5	46.3	1625	–
U3: L + Cr_7C_3 = ZrC + $Cr_{23}C_6$	18.2	80.9	0.9	1610	1605
E2: L = ZrC + $Cr_{23}C_6$ + (βCr)	13.8	85.4	0.8	1570	1575
E3: L = ZrC + C36 + (βCr)	0.4	80.9	18.7	1563	1587
U4: L + C36 = ZrC + C15	2.6	43.5	53.9	1560	–
E4: L = ZrC + C15 + (βZr)	0.6	27.7	71.7	1333	1320

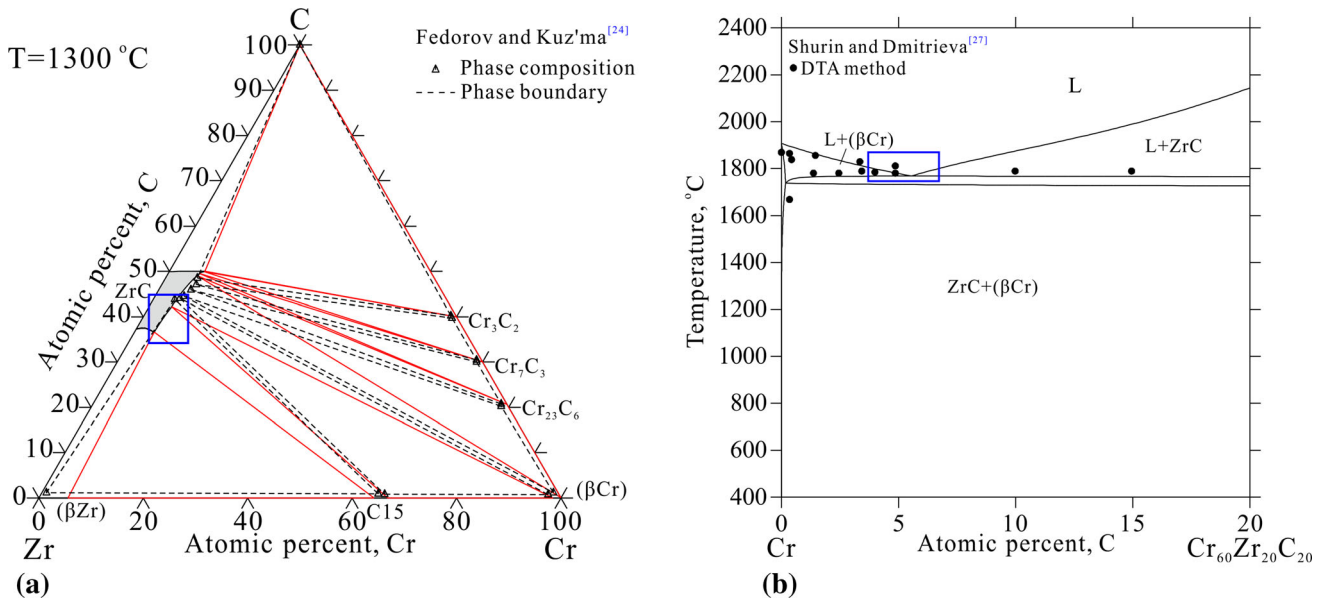

Fig. 7 Calculated isothermal section of 1300 °C and the Cr-ZrC vertical section, according to the remodeled parameters. The blue box indicates the worse fit between the calculated and experimental phase equilibria

Acknowledgments The financial support from the National Natural Science Foundation of China (51901063), the Fundamental Research Funds for the Central Universities of China (JZ2019HGBZ0114 and PA2020GDGP0054), the Program for Guangdong Introducing Innovative and Entrepreneurial Teams (2016ZT06G025) and Guangdong Natural Science Foundation (2017B030306014) is greatly acknowledged.

References

1. J.R. Li, P.F. Zhang, T. He, L.J. Cheng, L.W. Wang, and H. Li, Effect of carbides on high-temperature aging embrittlement in 12%Cr martensitic heat-resistant steel, *J. Mater. Res. Technol.*, 2019, **8**, p 5833-5846
2. T.K. Bandyopadhyay and K. Das, Processing and characterization of ZrC-reinforced steel-based composites, *J. Mater. Process. Tech.*, 2006, **178**, p 335-341
3. C.C. Lv, X.Y. Ren, C.B. Wang, and Z.J. Peng, Spark plasma sintering of ultrafine WC-10Ni-ZrC hardmetals: effects of adding ZrC nano-powder, *Int. J. Appl. Ceram. Technol.*, 2020, **17**, p 932-940
4. T. Lin, Y. Guo, Z. Wang, H.P. Shao, H.Y. Lu, F.H. Li, and X.B. He, Effects of chromium and carbon content on microstructure and properties of TiC-steel composites, *Int. J. Refract. Met. Hard Mater.*, 2018, **72**, p 228-235
5. J.O. Andersson, T. Helander, L. Hoglund, P. Shi, and B. Sundman, Thermo-Calc and DICTRA, computational tools for materials science, *Calphad*, 2002, **26**(2), p 273-312
6. L. Zhang, I. Steinbach, and Y. Du, Phase-field simulation of diffusion couples in the Ni-Al system, *Int. J. Mater. Res.*, 2011, **102**(4), p 371-380
7. Y.B. Peng, Y. Du, P. Zhou, W.B. Zhang, W.M. Chen, L. Chen, S.Q. Wang, G.H. Wen, and W. Xie, CSUTDCC1—a thermodynamic database for multicomponent cemented carbides, *Int. J. Refract. Metals Hard Mater.*, 2014, **42**, p 57-70
8. J.O. Andersson, Thermodynamic properties of Cr-C, *Calphad*, 1987, **11**, p 271-276
9. M. Kajihara and M. Hillert, Thermodynamic evaluation of the Cr-Ni-C system, *Metall Trans. A*, 1990, **21A**, p 2777-2787
10. B.-J. Lee, Thermodynamic assessment of the Fe-Nb-Ti-C-N system, *Metall. Mater. Trans. A*, 2001, **32A**, p 2423-2439
11. A.V. Khvan, B. Hallstedt, and K. Chang, Thermodynamic assessment of Cr-Nb-C and Mn-Nb-C systems, *Calphad*, 2012, **39**, p 54-61
12. V.N. Eremenko, T.Y. Velikanova, and A.A. Bondar, Phase diagram of the Cr-Mo-C system. I. Phase equilibria in the area of crystallization of alloys of the Mo-Mo_2C-Cr_7C_3-C partial system, *Poroshk. Metall.*, 1987, **293**, p 70-76
13. A.F. Guillermet, Analysis of thermochemical properties and phase stability in the zirconium-carbon system, *J. Alloys Compd.*, 1995, **217**(1), p 69-89
14. R.V. Sara, The system zirconium-carbon, *J. Am. Ceram. Soc.*, 1965, **48**(5), p 243-247
15. L.M. Adelsberg, L.H. Cadoff, and J.M. Tobin, Group IVB and VB metal carbide-carbon eutectic temperatures, *Trans. Metall. Soc. AIME*, 1966, **236**, p 972-977
16. E. Rudy, *Ternary Phase Equilibria in Transition Metal-Boron-Carbon-Silicon Systems. Part 5*. Comprendium of Phase Diagram Data, Air Force Materials Laboratory, WrightPatterson AFB, 1969, p 165–167
17. E.K. Storms and J. Griffin, Vaporization behavior of the defect carbides. IV. The zirconium-carbon system, *High Temp. Sci.*, 1973, **5**, p 291-310
18. L. Kaufman and H. Nesor, Treatise on Solid State Chemistry, Plenum Press, 1975
19. T. Chart and F. Putland, Thermodynamically calculated phase-diagram for the Co-Cr-Zr system, *Calphad*, 1979, **3**, p 9-18
20. K. Zeng, C. Haemaelaeinen, and R. Luoma, A thermodynamic assessment of the Cr-Zr system, *Z. Met.*, 1993, **84**, p 23-28
21. J. Pavlů, J. Vřeštál, and M. Šob, Stability of laves phases in the Cr-Zr system, *Calphad*, 2009, **33**, p 382-387
22. H.-J. Lu, W.-B. Wang, N. Zou, J.-Y. Shen, X.-G. Lu, and Y.-L. He, Thermodynamic modeling of Cr-Nb and Zr-Cr with extension to the ternary Zr-Nb-Cr system, *Calphad*, 2015, **50**, p 134-143

23. Y.L. Liu, P. Zhou, S.H. Liu, and Y. Du, Experimental investigation and thermodynamic description of the Cu-Cr-Zr system, *Calphad*, 2017, **59**, p 1-11
24. T.F. Fedorov and Y.B. Kuzma, Phase equilibria in the zirconium-chromium-carbon system, *Poroshk. Metall.*, 1965, **3**, p 75-79
25. V.N. Eremenko, T.Y. Velikanova, S.V. Sleptsov, and A.A. Bondar, Melting diagram of the Cr-Zr-C system, *Dokl. Akad. Nauk Ukrain. SSR*, 1990, **A**(1), p 70-72
26. V.N. Eremenko, T.Ya. Velikanova, S.V. Sleptsov, and A.A. Bondar, Phase equilibria at subsolidus temperatures and solidification behaviour of Cr-Zr-C alloys, *Metally*, 1992, **5**, p 144-150
27. A.K. Shurin and G.P. Dmitrieva, Phase diagrams of the Cr-HfC and Cr-ZrC system, *Akad. Nauk Ukr. SSR Metallofizika*, 1974, **51**, p 105-109
28. A.T. Dinsdale, SGTE data for pure elements, *Calphad*, 1991, **15**(4), p 317-425
29. O. Redlich and A.T. Kister, Thermodynamics of nonelectrolytic solutions. Algebraic representation of thermodynamic properties and the classification of solutions, *Ind. Eng. Chem.*, 1948, **40**, p 84-88
30. Y.M. Muggianu, M. Gambino, and J.P. Bros, Enthalpies of formation of liquid alloys bismuth-gallium-tin at 723° K. Choice of an analytical representation of integral and partial excess functions of mixing, *J. Chim. Phys. Phys. Chim. Biol.*, 1975, **72**(1), p 83-88
31. M. Hillert and M. Jarl, A model for alloying effects in ferromagnetic metals, *Calphad*, 1978, **2**, p 227-238
32. B. Sundman, B. Jansson, and J.O. Andersson, The thermo-calc databank system, *Calphad*, 1985, **9**, p 153-190
33. Y. Du, R. Schmid-Fetzer, and H. Ohtani, Thermodynamic assessment of the V-N system, *Z. Metallkd.*, 1997, **88**, p 545-556
34. J.C. Schuster and Y. Du, Thermodynamic description of the system Ti-Cr-C, *Calphad*, 1999, **23**, p 393-408
35. C.S. Sha, M.J. Bu, H.H. Xu, Y. Du, S.Q. Wang, and G.H. Wen, A thermodynamic modeling of the C-Cr-Ta ternary system, *J. Alloys Compd.*, 2011, **509**, p 5996-6003
36. Y.B. Peng, P. Zhou, M.J. Bu, W.B. Zhang, and Y. Du, A thermodynamic evaluation of the C-Cr-Nb system, *Calphad*, 2016, **53**, p 10-19